Hindawi
Wireless Communications and Mobile Computing
Volume 2022, Article ID 3306661, 9 pages
https://doi.org/10.1155/2022/3306661

Research Article

Research and Application of Key Technologies of Ocean Virtual Scene Display Based on Digital Image

Xiaonan Ren, Jie Ning, and Joung Hyung Cho

Department of Marine Design Convergence Engineering, Pukyong National University, Busan 48513, Republic of Korea Xiaonan

Correspondence should be addressed to Xiaonan Ren; xiaonan77@pukyong.ac.kr
and Joung Hyung Cho; 202056741@pukyong.ac.kr

Received 5 January 2022; Revised 11 February 2022; Accepted 4 April 2022; Published 3 June 2022

Academic Editor: Liqin Shi

Digital imaging technology originated from scientific and technological competitions in the military field, allowing continuous high-intensity digital photography work. The ocean virtual scene display of digital images is more flexible and more tolerant. The ocean virtual scene can be used to model the structure of different regions, create a diversified ocean experience pavilion as much as possible, and create a multi-dimensional visual product. Through this research, we get: 1. The best frame rate is 100.607 when High Dynamic Range (HDR) is off and 98.47 when HDR is on. When A =0.0161, Me =26, K1 = 0.6488, G =28, K2 = -0.0072, α =58, Omega =2.5229, β =78. The simulation experiment of ocean scene construction shows that it only needs to calculate the ocean virtual scene of LONC area, and repeatedly set and splice the ocean virtual scene to form a large modeling scene. 2. When the FFT model is optimized, the parameters are set as follows: Meta Flight =0.946, Open Flight =0.441, α =0.828, Omega =089, β =0.754; The optimal parameters of multiple kernel learning model in ocean virtual scene are: Meta Flight =0.757, Pen Flight =0.818, α =0.781, Omega =0.157, β =1.739; The best parameters of the ocean virtual scene of Vega Prime model are: Meta Flight =0.285, Open Flight =0.803, α =0.701, Omega =0.725, and β =0.757. And the constructed ocean virtual scene can achieve the best effect. 3. In the FFT model, when the related technical parameters are set optimally, the two-dimensional animation is integrated into the digital image as a visual special effect element or an animation subtitle, so that the digital image is more interesting, creative and propagable.

1. Introduction

Digital imaging technology originated from scientific and technological competitions in the military field. In the initial development period of digital imaging, this technology was mainly used in military fields such as aerospace and navigation. Digital imaging is significantly different from traditional film. The former is based on the photosensitive component Complementary Metal Oxide Semiconductor (CMOS), which can carry out continuous and high-intensity digital photography. Compared with traditional film imaging, the technical means are relatively backward and require a lot of manual operation. The requirements are high, and high-throughput work cannot be achieved. The development of digital imaging benefits from the development of Charge-coupled Device (CCD). Charge-coupled devices are used as storage devices [1–3]. Later, it was developed and applied in the field of digital imaging combined with photoelectric effect for storage of video effects. CMOS and CCD are continuously polished and updated to perfectly match the digital image. Digital imaging technology can help people understand the aesthetics of digital art, starting from the digital imaging features of human interaction. Digital imaging technology is a digital imaging art with digitization as the core. Its development may have an impact on the form of traditional imaging. However, the audience for digital imaging and traditional imaging is different and may reduce the huge contrast brought about by the impact. Digital photography technology has accelerated the human society from the writing age into the prosperous ocean virtual scene display, which greatly broadens the human visual experience. The creative form and scene construction are also more exaggerated and bold. The marine virtual scene display combines people and the machine has changed the traditional aesthetic feeling and way of aesthetics. Have a stronger sense of participation [4–8]. In the field of

computer and information science, influence interaction can be understood as "human-computer interaction" or the transmission of information back and forth. Interaction can also be interpreted as a two-way communication between the media and users, which can realize information interaction in the true sense. In a diversified network platform, digital images are the main form of information dissemination today, and digital images are used to promote the company's image and brand. At the beginning of its release, the Mi 11 Ultra reached the top of the professional imaging evaluation agency DXOMARK list. Mi 11 Ultra uses a 1/1.12-inch GN2 sensor with an ultra-outsole, which has been appreciated by users in both photography and video shooting. In addition to improving the picture quality, mobile phones must also consider the user's experience and interactive experience. The application of AI algorithms in photography and the needs of beauty are all user needs. For digital photography, anti-shake technology and high-resolution image quality The increase in rate, combined with technologies such as optical image stabilization, can significantly improve the digital camera experience of mobile phones. The 5G era and short video complement each other and promote the development of digital photography technology. 5G technology is of great help to the cloud platform technology of sports cameras. The video transmission quality of drones can reach high frame rates and 8 K images. Virtual technology combines 3D scanners, thermal imagers, and surveying instruments to form a framework of digital influence. Digital photography technology accelerates the human society from the writing age into the present prosperous ocean virtual scene display, which greatly broadens the visual experience and has a revolutionary change. With the great development of the marine virtual scene field [9, 10]. More and more people prefer virtual technology to experience some scenes, and virtual technology that can be close to the real experience is more popular. With its unique visual effects, the combination of ocean virtual scenes and real shot videos still has a lot of space and more forms of expression under different carriers and network communication methods. The advancement of virtual scene technology has made the production of 3D animation and digital special effects more and more realistic. The international and domestic markets are generally pursuing the production of 3D animation and film and television special effects. The traditional form of ocean scenes combined with video has encountered bottlenecks in the development and innovation of film forms, and it is difficult to make new breakthroughs. The ocean virtual scene display of digital images is more flexible and tolerant. The ocean virtual scene can be used to model and construct different regions, build a diversified ocean experience pavilion as much as possible, and tap more ocean dynamic elements to apply to reality. Take a video. The art form of inserting the ocean virtual scene into the real shot video is unique [11–15]. The flexible drawing style and the freely changing visual space, if used properly, will form a unique ocean virtual scene display, creating a multi-dimensional visual product. Insert some two-dimensional animations into the construction of ocean virtual scenes, and integrate two-dimensional animations as a kind of visual special effects elements or animated subtitles into digital images, making digital images more interesting, creative, and spreading wider. Although real ocean scenes and digital photography have more perfect viewing visual effects, the production of complex underwater worlds and large aquariums requires a long period of time for animal needs, and the investment in money and time is still large. Video works in the era of digital imaging pay more attention to the speed of dissemination and the evaluation and influence of audience groups than in the past. However, the combination of traditional animation films has lacked freshness for today's audiences. Combine two-dimensional animation with real shot video, explore more ways to combine the two and the effect of combining different real shot video content, both in terms of visual performance of the video and production cost, it is a win-win situation s Choice.

2. Digital Imaging Technology and Virtual Scene Construction Technology

2.1. Digital Imaging Technology. Digital video is the use of a video camera to transform the real world under the ocean into electrical signals, which are images recorded in digital form. The development of imaging technology is divided into traditional imaging technology and digital imaging technology. With the help of the fermentation of today's network environment, digital images have formed digital images of production methods, digital images of storage methods, and digital images of broadcast methods. The carrier of digital images is digital photography equipment, which can record and output optical and electrical signals. Figure 1 shows the main framework of imaging technology [16].

2.2. Storage and Transmission of Digital Images. As shown in Figure 2, the process of storing and transmitting digital images is visualized. Digital image storage devices include digital tapes, digital P2 cards, digital Blu-ray discs and digital disks, which are spread through network video streams, and finally form a network pandemic to achieve the final flow realization purpose. In the creation of digital video, two-dimensional animation can be used for creation, which brings together the advantages of animation software, and the blessing of a computer can definitely contribute to the effect and quality of the film. The digital camera shoots the scene as an entity and can record the truest side of the world. Two-dimensional animations are relatively weak, and sometimes they cannot achieve perfect presentation effects due to different perspectives. Digital imaging has interactive functions in the field of digital art, and can be used to build ocean virtual scenes by combining computer and information science, communication, aesthetics, and psychology. The interaction of the ocean virtual scene is "to realize the expression of artistic concepts through the artistic expression method of ocean virtual and the way of virtual scene construction mode.

2.3. Digital Interaction. The interaction of the ocean virtual scene includes four levels, including: viewing on the spot, browsing on the network, using virtual equipment for experience, and on-site control. As an art form supported by digital technology, the ocean virtual scene art of digital imaging is a powerful expansion of interaction. After all, pure VR viewing cannot achieve the immersive experience. Only when the experiencer decides the direction of things in the

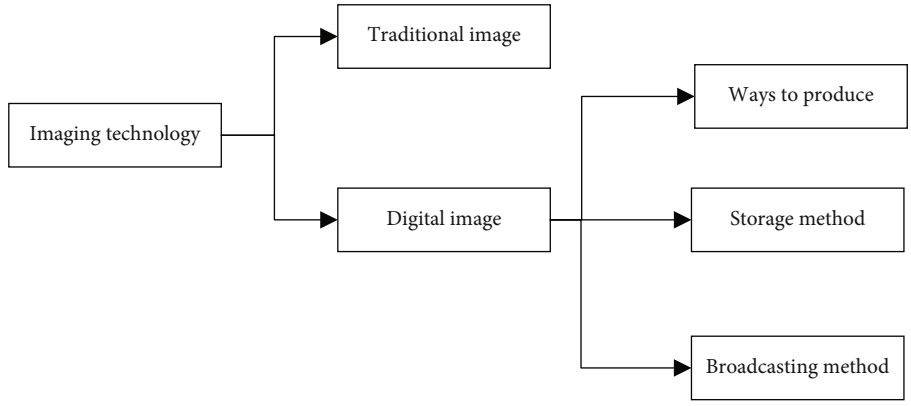

Figure 1: Image technology.

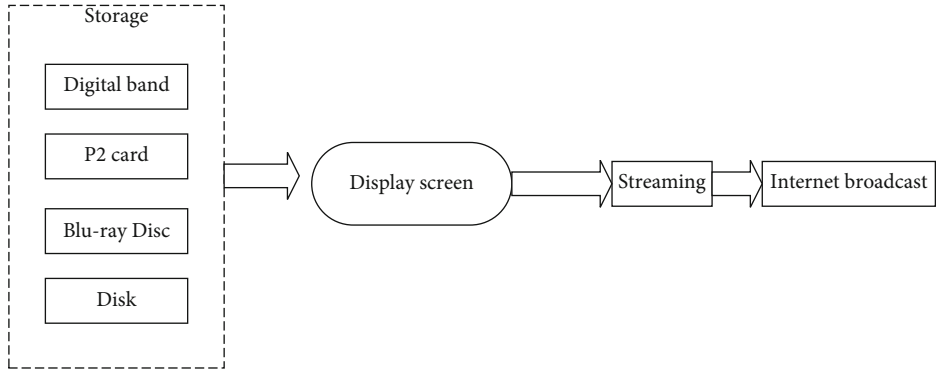

Figure 2: Storage and transmission of digital images.

virtual world, can they control and change the direction of things in virtual modeling. This lies in the digital interactive magic of ocean virtual scenes, which can truly be expressed as aesthetic activities. In digital art, its essence has not changed, because the law of communication of interaction is the same, and the difference is only the innovation and breakthrough in the degree of interaction between content and form. The interactivity of digital art is a way of making use of specific information transmission equipment and feedback systems in the virtual environment of the Internet platform to carry out the individualized participation of people and people, people and works, and people and systems.

2.4. Target Detection Algorithm. R-CNN (Regions with CNN features or Region-based Convolution Neural Networks) is an A region-based convolutional neural network algorithm. Traditional art cannot provide audiences with a platform for interactive aesthetic manipulation of virtual ocean scenes due to the limitations of technical conditions, appreciation experience, and form. Customers who visit the aquarium will not have a sense of participation in art. The spread of digital ocean virtual scenes has linear characteristics, so that customers of the aquarium can personally participate in the process of art formation. Under the conditions of rapid development of digital technology, the strategic phenomenon of regional recommendation has been changed, and mastering digital technology has become a target positioning model. In the formation of a bottom-up art acceptance process, the audience broke through the single, one-way passive aesthetic method of traditional target detection algorithms, and instead focused on the selection and control of multi-scale sliding, and mastered the target. The initiative of regional artistic aesthetics. R-CNN abandons the traditional ocean virtual scene idea, creatively combines the ocean virtual scene with CNN, and finally makes the construction speed of the ocean virtual scene and the speed and accuracy of target detection have been significantly improved.

Table 1: FFT transform method.

Frame rate	HDR off	HDR on	Lonc	Latc
Frame rate at that time	93.569	81.267	95.429	88.32
Average frame rate	95.429	83.591	95.769	89.65
Worst frame rate	90.769	74.629	82.32	96.65
Optimal frame rate	100.607	98.476	96.23	84.65

3. Application of Digital Images in Ocean Virtual Scenes

(a) FFT [17–20]

Digital image

$$\alpha^T = [a_0, a_1, \cdots, a_{n-1}] \quad (1)$$

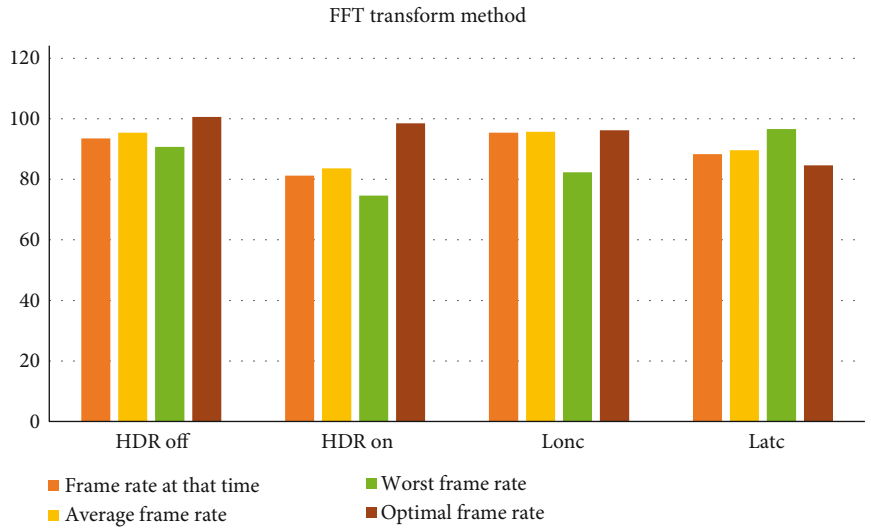

Figure 3: FFT transform method.

$$P_a(x) = \sum_{i=0}^{n-1} a_i x^i \tag{2}$$

Digital image storage method

$$P_a(x) = Xa^T \tag{3}$$

$$X^T = \left[1, x, x^2, \cdots, x^{n-1}\right] \tag{4}$$

Digital video broadcast method

$$P_a = \Omega a \tag{5}$$

Ocean virtual scene

$$P(x) = a_0 + a_1 x + a_2 x^2 + a_3 x^3 + \cdots + a_{n-1} x^{n-1} \tag{6}$$

MKL [21–23]

$$P_e\left(x^2\right) = a_0 + a_2 x^2 + a_4 \left(x^2\right)^2 + \cdots + a_{n-2} x^{n-2} \tag{7}$$

Equipment for experience

$$xP_e\left(x^2\right) = x\left[a_0 + a_2 x^2 + a_4 \left(x^2\right)^2 + \cdots + a_{n-2} x^{n-2}\right] \tag{8}$$

On-site control

$$P(x) = P_e\left(x^2\right) + xP_e\left(x^2\right) \tag{9}$$

$$P_e(x) = a_0 + a_2 x + a_4 x^2 + \cdots + a_{n-2} x^{n-2/2} \tag{10}$$

$$P_{ee}(x) = a_0 + a_2 x + a_8 x^4 + \cdots + a_{n-4} x^{n-2/2-1} \tag{11}$$

$$xP_{ee}(x) = x\left[a_0 + a_2 x + a_8 x^4 + \cdots + a_{n-4} x^{n-2/2-1}\right] \tag{12}$$

Table 2: Scene simulation.

NO	Wind speed	Fetch length
a	5 m/s	1500 km
b	10 m/s	50 km
c	10 m/s	500 km
d	15 m/s	1500 km
e	20 m/s	50 km
f	20 m/s	750 km
g	20 m/s	1500 km

Table 3: Construction of ocean scene.

NO	A	Me	K1	G	K2	α	Omega	β
1	0.0161	26	0.6488	28	-0.0072	58	2.5229	78
2	0.0064	89	2.1143	85	-0.0092	66	4.5544	45
3	0.0161	26	0.648	89	-0.0317	83	2.5229	78
4	0.0196	39	0.8359	95	0.03301	51	2.8648	81
5	0.0104	35	0.4084	78	-0.0528	72	2.0101	24
6	0.0104	35	0.4011	65	0.09335	27	2.0101	24
7	0.0033	9	0.6375	48	-0.1206	75	2.5229	78
8	0.0027	77	4.3809	62	-0.1211	18	6.5574	53
9	0.0011	35	7.0132	27	11.2821	93	11.423	35
10	0.0008	94	10.506	58	-12.154	21	12.566	71
11	0.0008	94	-10.06	56	-12.522	26	12.566	71
12	0.0011	35	-3.257	49	12.8787	35	11.423	35
13	0.0011	35	-2.383	69	13.0687	22	11.423	35
14	0.0011	35	0.4647	67	13.2761	58	11.423	35
15	0.0008	94	6.5805	79	14.6564	24	12.566	31
16	0.0008	94	-5.686	83	15.0257	75	12.566	71
17	0.0008	94	1.8399	31	15.9602	27	12.566	31

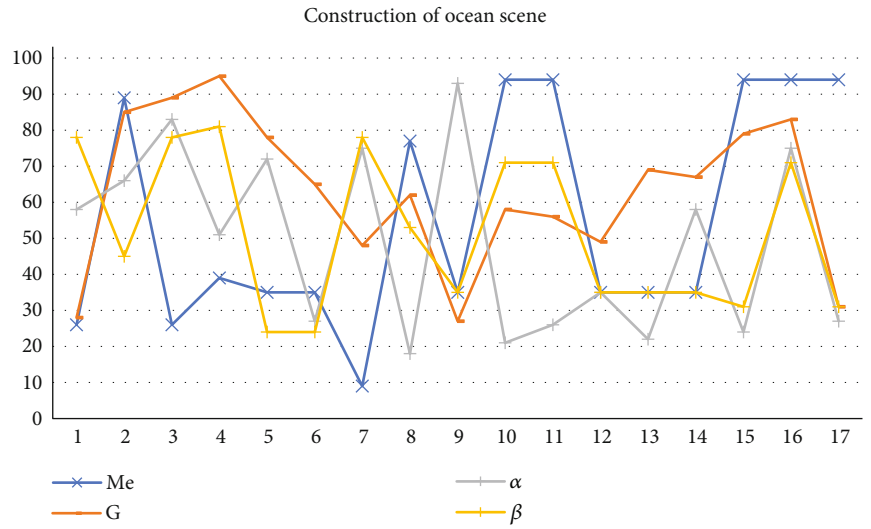

Figure 4: Construction of ocean scene.

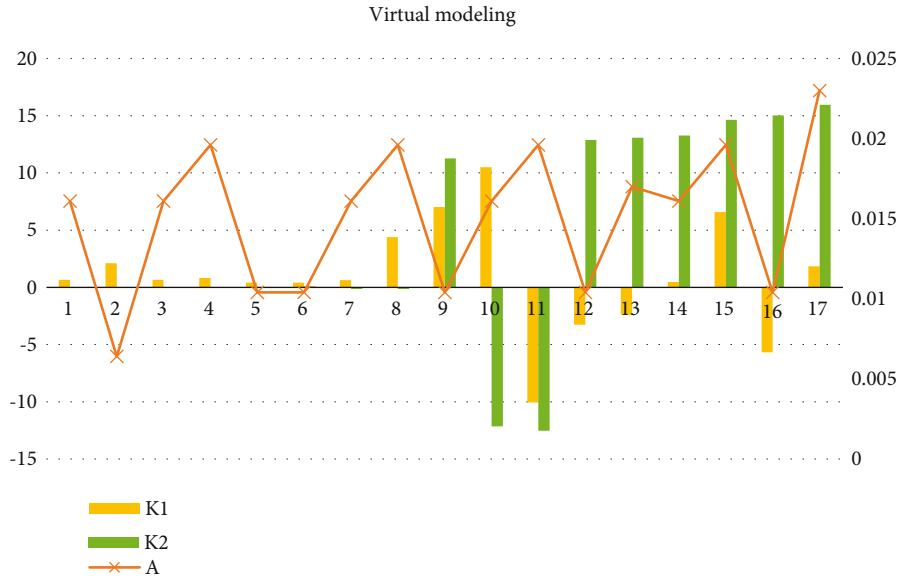

Figure 5: Virtual modeling.

Sea wave crest

$$P_e(x) = P_{ee}(x^2) + xP_{eo}(x^2) \tag{13}$$

$$P_o(x) = P_{oe}(x^2) + xP_{oo}(x^2) \tag{14}$$

$$n \in \{\omega_n^0, \omega_n^1, \cdots, \omega_n^{n-1}\} \tag{15}$$

The wave crest is sharper. Database operation based on XML data scene

$$P(\omega_n^k) = P_e(\omega_n^{2k}) + \omega_n^k P_0(\omega_n^{2k}) \tag{16}$$

Where $k = 0, 1, \cdots, n-1$.

Table 4: Comparison of model parameters.

FFT	MKL	Vega prime	Meta flight	Open flight	α	Omega	β
0.256	0.443	0.192	0.946	0.441	0.828	0.089	0.754
0.807	0.353	0.913	0.823	0.893	0.598	0.365	0.348
0.557	0.701	0.725	0.757	0.818	0.781	0.157	0.739
0.222	0.976	0.764	0.78	0.724	0.866	0.744	0.751
0.841	0.776	0.557	0.256	0.782	0.353	0.913	0.823
0.876	0.235	0.222	0.285	0.803	0.701	0.725	0.757
0.247	0.369	0.773	0.634	0.589	0.752	0.88	0.461

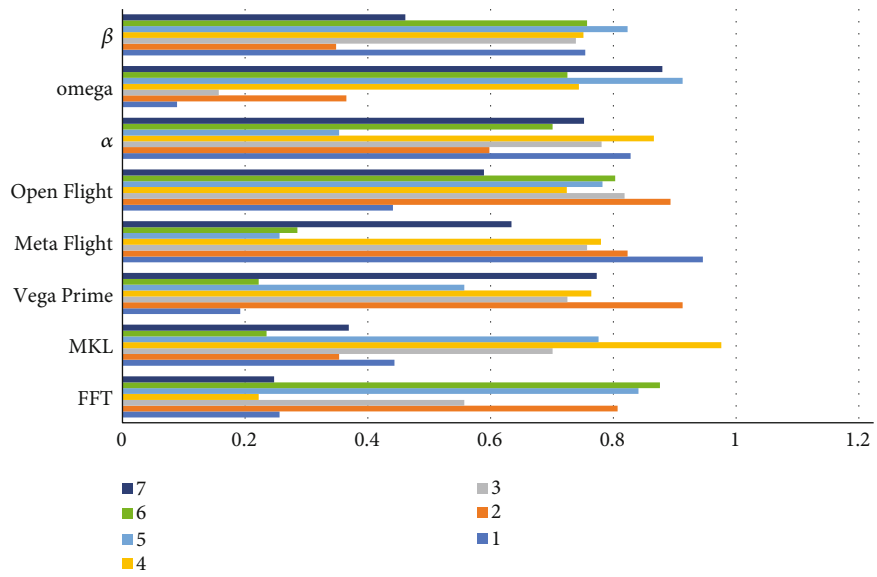

Figure 6: Comparison of model parameters.

C.Vega Prime [24, 25]

$$P\left(\omega_n^k\right) = P_e\left(\omega_{n/2}^{2k}\right) + \omega_n^k P_0\left(\omega_{n/2}^{2k}\right) \tag{17}$$

Where $k = 0, 1, \cdots, n/2 - 1$.

$$d = \frac{\sqrt{3}}{2}a \tag{18}$$

$$d \le Z_{far} \tag{19}$$

Flat trough

$$r_{x_1} = \frac{(x_1/d \cdot \tan(fov/2)) + 1}{2} \cdot r_{width} \tag{20}$$

$$r_{x_2} = \frac{(x_2/d \cdot \tan(fov/2)) + 1}{2} \cdot r_{width} \tag{21}$$

$$r_{x_2} - r_{x_1} = 1 \tag{22}$$

Ocean virtual scene wave Open Flight application range

$$\frac{(x_1/d \cdot \tan(fov/2)) + 1}{2} - \frac{(x_2/d \cdot \tan(fov/2)) + 1}{2} \cdot r_{width} = 1 \tag{23}$$

$$x_2 - x_1 = 2d\frac{\tan(fov/2)}{r_{width}} \tag{24}$$

$$T_{x_1} = \frac{(x_1/d) + 1}{2} \cdot T_{size} \tag{25}$$

Table 5: Marine virtual scene modeling.

Parameter	FFT	MKL	Vega prime
Me	52.08	25.12	15.76
K1	52.33	33.81	17.52
G	55.01	35.41	10.34
K2	40.22	26.88	36.08
α	31.02	38.20	12.66
Omega	34.61	32.71	10.31
β	45.93	44.31	21.91
Me2	38.00	37.68	15.94
K3	34.20	35.32	17.61
G2	45.42	24.83	32.68
K4	35.84	33.15	19.87
J	46.23	40.79	18.01
omega2	37.73	32.06	38.01
β2	39.35	31.81	12.02
M2	40.96	25.70	36.26
P2	42.47	21.38	13.43
t2	45.02	23.60	21.27

Model simulation under different wind speeds

$$T_{x_2} - T_{x_1} = 1 \tag{26}$$

$$x_2 - x_1 = \frac{2d}{T_{size}} \tag{27}$$

$$T_{size} = \frac{R_{width}}{\tan(fov/2)} \tag{28}$$

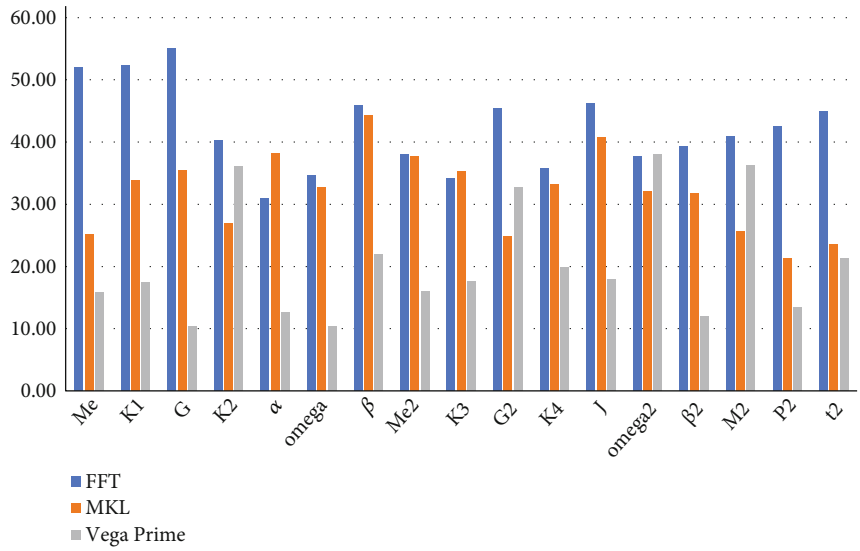

Figure 7: Comparison of model architecture.

4. Simulation Experiment

4.1. FFT Transform Method. The FFT transform method (shown in Table 1 and Figure 3) for modeling and simulation of ocean virtual scenes can improve the image presentation effect of the superposition method based on ocean waves. For the evaluation of modeling and simulation of ocean virtual scenes, The dispersibility of the plane ripple and the continuous sine wave are brought into the evaluation index. The FFT transform method can expand the virtual scene of the ocean. When HDR is turned off, the frame rate at that time =93.569, the average frame rate =95.429, the worst frame rate =90.769, and the optimal frame rate =100.607. When HDR is turned on, the current frame rate =81.267, the average frame rate = 81.26, the worst frame rate = 83.59, and the optimal frame rate = 98.47. Latc increased the frame rate of the simulation to 95.42 and the rendering speed to 89.65. The FFT average frame rate transformation has a periodicity of 96.65, so the worst frame rate is 84.65. There is no need to increase the calculation of grid nodes. Only the ocean virtual scene in the lonc area needs to be calculated, and this ocean virtual scene is repeatedly set and spliced to form a large modeling scene.

4.2. Vega Prime 3D Scene Simulation. Vega Prime has a powerful horizontal correction feature, users can control the correction factor on multiple platforms, and realize Meta Flight cross-platform operation. Meta Flight can increase the sea surface wave crest, the wave crest is sharper and the database operation based on XML data scene, the flatter shape of the wave trough can better play the operation of the database, ocean virtual scene, etc. The wave greatly expands the Open when the sea condition is high. Flight application range. The model simulation under different wind speeds is shown in Table 2, which can simulate the roll of sea waves.

4.3. Construction of Ocean Scene. Set the scene parameter A to be tidal force, M to wave crest, K1 to zp112 test, G to surface heat, K2 to groundwater, α to represent ground wind, omega to sea velocity, and β to surface wind. In the simulation experiment, the first group showed A =0.0161, Me =26, K1 = 0.6488, G =28, K2 = -0.0072, α =58, omega =2.5229, β =78. In the fifth optimization, A = 0.0104, Me = 35, K1 = 0.4084, G = 78, K2 = -0.0528, α = 72, omega = 2.0101, β = 24; when N = 15, A = 0.0008, Me = 94, K1 = 10.506, G =58, K2 = -12.154, α = 21, omega = 12.566, β = 71; N = 17 is the best A = 0.0008, Me = 94, K1 = 1.8399, G = 31, K2 = 15.9602, A = 27, omega = 12.566, β = 31. As shown in Table 3 and Figures 4 and 5.

4.4. Comparison of Model Parameters. The FFT model, MKL model, and Vega Prime model are simulated and compared, and the results are shown in Table 4 and Figure 6. In the FFT model, Meta Flight, Open Flight, α, mega, and β parameters are used for evaluation. The best parameters of the FFT model are Meta Flight =0.946, Open Flight =0.441, α =0.828, omega = 0.089, β =0.754; the best parameters of MKL are: Meta Flight =0.757, pen Flight =0.818, α =0.781, omega =0.157, β = 0.739; the best parameters of the Vega Prime model are Meta Flight =0.285, Open Flight =0.803, α =0.701, omega =0.725, β =0.757.

Insert some two-dimensional animations into the construction of the ocean virtual scene, as shown in Table 5, Figure 7, and Figure 8. In the FFT model, Me = 52, K1 = 52, G = 55, K2 = 40, α = 31, omega = 35, β = 46, Me2 = 38, K3 = 34, G2 = 45, K4 = 36, J = 46, omega2 = 38, β2 = 39, M2 = 41, P2 = 42, t2 = 45. Two-dimensional animation is integrated into digital images as a kind of visual special effects elements or animated subtitles, making digital images more interesting, creative, and spreading wider. In the MKL model, Me = 25, K1 = 34, G = 35, K2 = 27, α = 38, omega = 33, β = 44, Me2 = 38, K3 = 35, G2 = 25, K4 = 33, J = 41, omega2 = 32, β2 = 32, M2 =26, P2 = 21, t2 = 24; in the Vega Prime model, Me = 16, K1 = 18, G = 10, K2 = 36, α = 13,

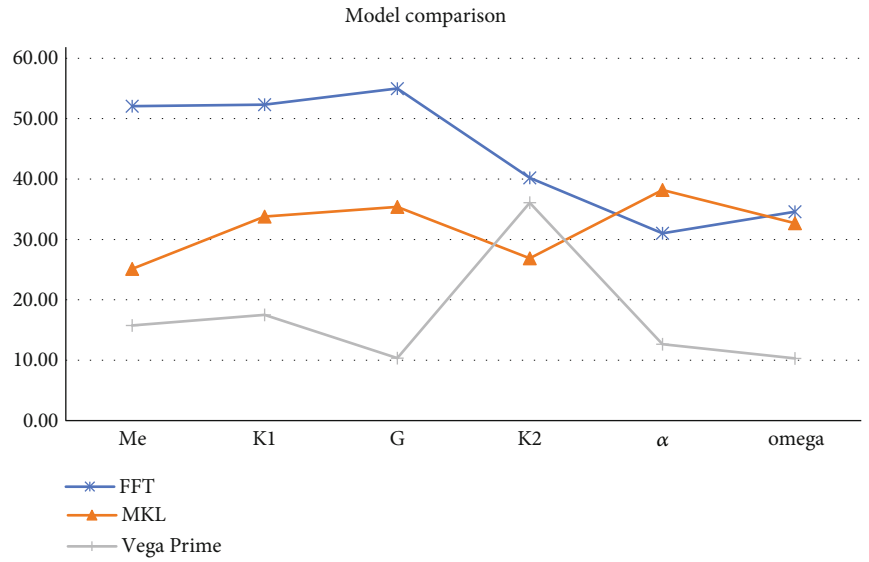

Figure 8: Model comparison.

omega = 10, $\beta = 22$, Me2 = 16, K3 = 18, G2 = 33, K4 = 20, J = 18, omega2 = 38, $\beta 2 = 12$, M2 = 36, P2 = 13, t2 = 21.

From Figure 8, FFT has high execution time and poor performance under different indexes. While MKL is at a general level, it has certain advantages over FFT as a whole. The Vega Prime model has good performance, can achieve lower execution time, for the other two models, the advantage is more obvious.

5. Conclusion

The ocean virtual scene display of digital images is more flexible and more tolerant. The ocean virtual scene can be used to model the structure of different regions, create a diversified ocean experience pavilion as much as possible, and create a multi-dimensional visual product. Two-dimensional animation is integrated into digital images as a kind of visual special effects elements or animated subtitles, making digital images more interesting, creative, and spreading wider. Digital image of the ocean virtual scene has a good application scene, can be applied to multi-dimensional visual effects. Using big data parallel processing technology to quickly analyze related features and improve analysis accuracy. It can be applied comprehensively from different feature attributes for different scenes, and reflects the complex application of digital images in marine virtual scenes.

Data Availability

The experimental data used to support the findings of this study are available from the corresponding author upon request.

Conflicts of Interest

The authors declared that they have no conflicts of interest regarding this work.

Acknowledgments

This work was supported by a grant from Brain Korea 21 Program for Leading Universities and Students (BK21 FOUR) MADEC Marine Designeering Education Research Group.

References

[1] M. D. Presnar, A. D. Raisanen, D. R. Pogorzala, J. P. Kerekes, and A. C. Rice, "Dynamic scene generation, multimodal sensor design, and target tracking demonstration for hyperspectral/Polarimetric performance-driven sensing," *Proceedings of SPIE-The International Society for Optical Engineering*, vol. 7672, article 76720T, 2010.

[2] J. A. Rupkalvis and R. Gillen, *A New Method for Combining Live Action and Computer Graphics in Stereoscopic 3D[C]// Engineering Reality of Virtual Reality*, International Society for Optics and Photonics, San Jose, CA(US), 2008.

[3] G. Zhang, C. Huang, J. Li, and X. Zhang, "Constrained coordinated path-following control for underactuated surface vessels with the disturbance rejection mechanism," *Ocean Engineering*, vol. 196, p. 106725, 2020.

[4] J. Liu, D. Chen, Y. Wu, R. Chen, P. Yang, and H. Zhang, "Image edge recognition of virtual reality scene based on multi-operator dynamic weight detection," *IEEE Access*, vol. 8, pp. 111289–111302, 2020.

[5] S. Alkahtani, A. Eisa, J. Kannas, and G. Shamlan, "Effect of acute high-intensity interval cycling while viewing a virtual natural scene on mood and eating behavior in men: A randomized pilot trial," *Clinical Nutrition Experimental*, vol. 28, pp. 92–101, 2019.

[6] K. Zhbanova, "Ocean underwater scene dioramas of first graders with submarine porthole views," *Journal of STEM Arts, Crafts, and Constructions*, vol. 4, no. 1, article 4, 2019.

[7] T. Sieberth, A. Dobay, R. Affolter, and L. C. Ebert, "Applying virtual reality in forensics - a virtual scene walkthrough," *Forensic Science Medicine & Pathology*, vol. 15, no. 1, pp. 41–47, 2019.

[8] M. Liao, B. Song, S. Long, H. E. Minghang, C. Yao, and X. Bai, "SynthText3D: synthesizing scene text images from 3D virtual worlds," *SCIENCE CHINA Information Sciences*, vol. 63, no. 2, pp. 1–14, 2020.

[9] X. Ning, P. Duan, W. Li, and S. Zhang, "Real-time 3D face alignment using an encoder-decoder network with an efficient deconvolution layer," *IEEE Signal Processing Letters*, vol. 27, pp. 1944–1948, 2020.

[10] A. Bayramova, T. Mane, T. Ogunleye, S. C. Taylor, and E. Bernardis, "Photographing alopecia: how many pixels are needed for clinical Evaluation?," *Journal of Digital Imaging*, vol. 33, no. 6, pp. 1404–1409, 2020.

[11] N. P. Dang, K. Chandelon, I. Barthélémy, L. Devoize, and A. Bartoli, "A proof-of-concept augmented reality system in oral and maxillofacial surgery," *Journal of stomatology Oral and Maxillofacial Surgery*, vol. 19, no. 1, pp. 338–342, 2021.

[12] G. B. Chen, Z. Sun, and L. Zhang, "Road identification algorithm for remote sensing images based on wavelet transform and recursive operator," *IEEE Access*, vol. 8, pp. 141824–141837, 2020.

[13] T. Fromenteze, O. Yurduseven, P. D. Hougne, and D. R. Smith, "Lowering latency and processing burden in computational imaging through dimensionality reduction of the sensing matrix," *Scientific Reports*, vol. 11, no. 1, pp. 1–14, 2021.

[14] G. Chen, L. Wang, and M. M. Kamruzzaman, "Spectral classification of ecological spatial polarization SAR image based on target decomposition algorithm and machine learning," *Neural Computing and Applications*, vol. 32, no. 10, pp. 5449–5460, 2020.

[15] B. Huber, D. Mcduff, C. Brockett, M. Galley, and B. Dolan, "Emotional dialogue generation using image-grounded language models," in *Proceedings of the 2018 CHI Conference on Human Factors in Computing Systems*, Montreal, QC, Canada., April 2019.

[16] J. Wang, Z. Li, W. Hu, Y. Shao, and Y. Chen, "Virtual reality and integrated crime scene scanning for immersive and heterogeneous crime scene reconstruction," *Forensic Science International*, vol. 303, article 109943, 2019.

[17] W. Li, L. Liu, and J. Zhang, "Fusion of SAR and optical image for sea ice Extraction," *Journal of Ocean University of China*, vol. 20, no. 6, pp. 1440–1450, 2021.

[18] K. Rahimi, C. Banigan, and E. D. Ragan, "Scene Transitions and Teleportation in Virtual Reality and the Implications for Spatial Awareness and Sickness," *IEEE Transactions on Visualization and Computer Graphics*, vol. 26, no. 6, pp. 2273–2287, 2018.

[19] T. C. Bybee and S. E. Budge, "Method for 3-D scene reconstruction using fused LiDAR and imagery from a Texel Camera," *IEEE Transactions on Geoscience and Remote Sensing*, vol. 57, no. 11, pp. 8879–8889, 2019.

[20] Y. Chen, D. Wang, and G. Bi, "An image edge recognition approach based on multi-operator dynamic weight detection in virtual reality scenario," *Cluster Computing*, vol. 22, pp. 8069–8077, 2019.

[21] N. Sarhangnejad, N. Katic, Z. Xia, M. Wei, and R. Genov, "Dual-tap computational photography image sensor with per-pixel pipelined digital memory for intra-frame coded multi-exposure," *IEEE Journal of Solid-State Circuits*, vol. 54, no. 11, pp. 3191–3202, 2019.

[22] M. Awad, A. Elliethy, and H. A. Aly, "Adaptive near-infrared and visible fusion for fast image enhancement," *IEEE Transactions on Computational Imaging*, vol. 6, pp. 408–418, 2020.

[23] M. A. Guang-Ming, C. H. Wang, and L. I. Li-Ning, "Based on CityEngine 3D virtual campus scene design and implementation," *Computer Engineering & Software*, vol. 63, no. 2, pp. 1–14, 2019.

[24] Z. Sunm, Y. Q. Liu, C. R. Zhang, J. Shi, and Y. Y. Chen, "A scene-distributed interactive rendering system," *Journal of Graphics*, vol. 3, no. 2, pp. 1–14, 2019.

[25] Y. Liu, L. Shen, G. Zhang, and F. Liu, "Design on virtual simulation experiment for digital teaching video shooting and evaluation in complex scene," *Experimental Technology and Management*, vol. 6, pp. 1–14, 2019.